Proceedings Paper:
Lone, J.A., Drummond, R., Bhaumik, S. et al. (2025) A discrete-time observer for parallel connected battery packs with nonlinear descriptor system dynamics. In: 2025 American Control Conference (ACC). 2025 American Control Conference (ACC), 08-10 Jul 2025, Denver, CO, USA. Institute of Electrical and Electronics Engineers (IEEE), pp. 4031-4036. ISBN: 9798350367614. ISSN: 0743-1619. EISSN: 2378-5861.

https://doi.org/10.23919/acc63710.2025.11107740

A Discrete-time Observer for Parallel Connected Battery Packs with Nonlinear Descriptor System Dynamics

Jaffar Ali Lone, Ross Drummond, Shovan Bhaumik and Nutan Kumar Tomar

***Abstract*— An observer is developed for the nonlinear descriptor system dynamics of parallel connected lithium-ion battery packs. The observer estimates the states of the individual cells in the pack with stability guarantees provided. When evaluated on the urban dynamometer driving schedule, the proposed observer performs well, with root mean squared errors (RMSEs) of 0.0072 and 0.0054 in the state-of-charges as well as $0.3A$ and $0.28A$ in the currents for cells 1 and 2, respectively. The results also demonstrated the value of incorporating busbar resistances in the model. In particular, with the inclusion of a busbar resistance of 0.02Ω, the mismatch in currents grew by 9.69% for cell 1 and by 8.55% for cell 2. These results highlight the potential of implementing cell-level state estimation and control in large battery packs accounting for cell-to-cell variability and busbar resistances.**

***Index Terms*— Descriptor systems, Parallel connected battery packs, State estimation, Stability analysis.**

I. Introduction

Without state-estimation, we would not have technologies such as electric vehicles (EVs). In fact, the impact of state-estimation, especially for the state-of-charge (SOC), in battery management systems (BMS), for alleviating driver range anxiety is, in retrospect, perhaps a somewhat underappreciated aspect behind the growth of EVs seen in recent years. The value of the BMS to electric technologies, such as EVs, has stimulated significant amounts of research on state-estimation for batteries, with an overview given in [1]. However, most of these works analysed individual cells rather than considering the specific features of the large battery packs powering the high energy/power electrified technologies of today. As lithium-ion battery packs get bigger (for example, there are approximately 7,104 cells in the 74P96S pack of the Tesla Model S), there is a growing need for algorithms tailored to address these pack-level considerations [2].

The next generation of electric technologies, notably electric aircraft, will require even more stringent BMS performance, as poor state estimates or undetected cell-faults could lead to serious consequences. These advanced applications are pushing forward research into algorithms able to estimate the states of *every* cell in the pack. The need for cell-level estimation is due to the fact that no two lithium-ion batteries are the same. Growing experimental evidence (e.g. [3]) is revealing the existence of significant variations between the parameters of the pack's cells, caused by differences in manufacturing and also in usage. These cell-to-cell parameter variations mean that every cell is unique, and so optimal performance of the BMS can only be achieved by exploiting this uniqueness rather than lumping the pack as a single entity as has been previously implemented [1], [4].

To implement cell-level state-estimation, the pack topology (as in how the cells are connected in series and parallel) must first be understood. For the purpose of state-estimation, parallel connections are arguably more challenging as the resulting pack dynamics are described by differential-algebraic equations (DAEs), or descriptor systems in discrete time, as Kirchhoff's laws must be enforced at every moment in time [5]. The DAEs of parallel packs can generate more complex dynamics; with current oscillations and SOC distributions [5]–[9]. By contrast, with series connections, each cell has the same current and so the state-estimation problem can be decoupled. As a consequence of their added complexity, there are still significant open research problems that need to be addressed before cell-level estimation of parallel connected packs can be implemented in the field.

Although substantial progress has been made in the observer design for nonlinear descriptor systems, most of these studies have considered continuous-time systems, such as [10]–[12]. In contrast, the observer design for discrete-time nonlinear descriptor systems has received relatively little attention. Existing results include [13]–[15] but all these methods have considered the nonlinearity only in the state equation and not in the output equation. Handling descriptor systems with nonlinearities present in both state and output equations can be challenging. This underscores the need for developing observers for nonlinear discrete-time descriptor systems.

Contributions

The main contributions of this paper are:

- A more general equivalent circuit model (ECM) of a parallel connected Li-ion battery pack is proposed through a nonlinear discrete-time descriptor system. This model goes beyond just capturing the basic electrical characteristics of the cells; it also explicitly accounts for the busbar resistance, which plays a critical role in the uneven current distribution among the cells.
- For the parallel connected battery pack, an observer is proposed for the state estimation targeting the SOC

Jaffar Ali Lone thanks the Ministry of Education, Govt. of India, for providing financial support via PMRF Grant no. 2701805.

Jaffar Ali Lone and Shovan Bhaumik are with the Department of Electrical Engineering, Indian Institute of Technology Patna, India. {jaffar_2121ee06,shovan.bhaumik}@iitp.ac.in.

Ross Drummond is with the Department of Automatic Control and Systems Engineering, University of Sheffield, UK. ross.drummond@sheffield.ac.uk.

Nutan Kumar Tomar is with the Department of Mathematics, Indian Institute of Technology Patna, India. nktomar@iitp.ac.in.

and local currents specifically. We also establish the conditions for the existence and stability of the proposed observer in terms of linear matrix inequalities (LMIs).
- The performance of the observer was evaluated on a discharge profile generated from the urban dynamometer driving schedule (UDDS) used in [16], with the observer's root mean squared errors (RMSEs) being 0.0072 and 0.0054 for the SOCs as well as 0.3A and 0.28A for the currents in cells 1 and 2, respectively, being obtained.

These results highlight the potential to implement cell-level state estimation in parallel connected packs with stability guarantees for the nonlinear descriptor system dynamics. Compared to existing results, such as [17], they demonstrate the value of including the observer gains as LMIs variables to optimise over. It is important to mention that the authors in [17] used a DAE-based observer for the cell level estimation of the pack. However, DAE observers are generally not preferable from the practical point of view because of their implicit nature and their need for consistent initial conditions during simulation. Moreover, the unconstrained observer dynamics involve derivatives of inputs and outputs and hence lead to ill-posed problems [11]. Compared to [9], the analysis is generalised to include bus-bar resistances as well as stability bounds. By exploiting the complexity from parallel pack connections, these results show how results from nonlinear descriptor system state-estimators could be used to implement cell-level state estimation.

II. Model Formulation of Parallel Connected Battery Pack

A. Cell model

Fig. 1 shows the second order Thevenin ECM of the m^{th} cell in a parallel connected module of n cells. In this paper, we utilize the ECM approach over the other methods (e.g. electrochemical models [4]) because it is relatively simple and has been experimentally validated [9]. Using the ECM of Fig. 1, the dynamics of the m^{th} cell in the parallel connected pack of n cells are

$$x_{m,k+1} = \tilde{A}_m x_{m,k} + \tilde{B}_m u_{m,k}, \tag{1a}$$

$$y_{m,k} = h_m(x_{m,k}) + \tilde{D}_m u_{m,k}, \tag{1b}$$

with $x_{m,k} = [Z_{m,k}\ V_{1m,k}\ V_{2m,k}]^T$ being the state vector at time step k, $Z_{m,k}$ the SOC, $V_{1m,k}$ and $V_{2m,k}$ the polarizing voltages of the RC pairs. The control input $u_{m,k} = I_{m,k}$ is the current, and $y_{m,k} = V_{Tm,k}$ is the terminal voltage of the m^{th} cell. The matrices $\tilde{A}_m$ and $\tilde{B}_m$ are parameterised by

$$\tilde{A}_m = \begin{bmatrix} 1 & 0 & 0 \\ 0 & e^{-\tau_{1m}} & 0 \\ 0 & 0 & e^{-\tau_{2m}} \end{bmatrix}, \tilde{B}_m = \begin{bmatrix} \frac{T_s}{C_{bm}} \\ R_{1m}(1-e^{-\tau_{1m}}) \\ R_{2m}(1-e^{-\tau_{2m}}) \end{bmatrix}.$$

and $\tilde{D}_m = [R_{0m}]$. Also, $h_m(x_{m,k}) = V_{OCV_{m,k}} + V_{1m,k} + V_{2m,k}$ with $V_{OCV_{m,k}}$ being the OCV which is a nonlinear function of the SOC. Here, $\tau_{1m} = \frac{T_s}{R_{1m}C_{1m}}$ and $\tau_{2m} = \frac{T_s}{R_{2m}C_{2m}}$. Moreover, R_0m represents the internal resistance, while R_{1m}, R_{2m}, C_{1m}, C_{2m} denote the polarization resistances and capacitances of the RC pairs for the m^{th} cell, respectively. C_{bm} is the battery capacity while T_s is the sampling time.

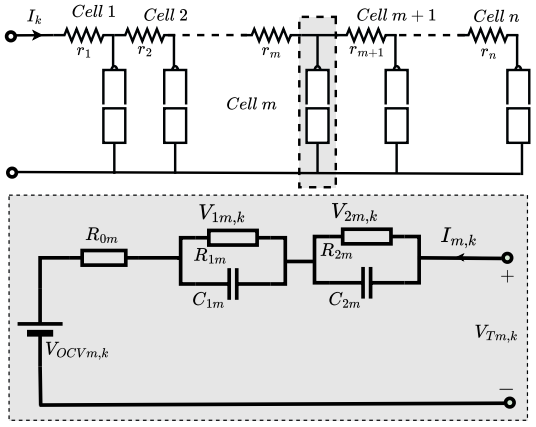

Fig. 1: Second order Thevenin ECM of m^{th} cell in a parallel connected module of n cells.

B. Pack model

Now, consider a module of n cells connected in parallel. In this analysis, we introduce an additional resistance, r_j, $j = 1,2,\cdots,n$, which accounts for the busbar resistance across the cells, as illustrated in Fig. 1. Incorporating this busbar resistance is crucial, as its variation can also lead to uneven current distribution among the cells, thereby providing a more accurate representation of the battery pack's real-world operational conditions [18]. This inclusion also distinguishes our model from the one presented in [17]. The dynamics of parallel connected packs are subject to Kirchhoff's laws, which enforce the conservation of current and voltage across the pack. Specifically, Kirchhoff's voltage law means that all the cells in the parallel pack have the same voltage with

$$\begin{aligned} &V_{OCV_{p,k}} + V_{1p,k} + V_{2p,k} + R_{0p}I_{p,k} \\ &\quad = V_{OCV_{q,k}} + V_{1q,k} + V_{2q,k} + R_{0q}I_{q,k} + r_q I_{q,k} \end{aligned} \tag{2a}$$

for all $p,q \in \{1,2,...,n\}$. Kirchhoff's current law imposes the total current flowing into each cell, with the notation $I_{j,k}(t)$ referring to the current flowing into cell j at time-step k, equals that applied to the pack, referred to as I_k, as in

$$\sum_{j=1}^{n} I_{j,k} = I_k. \tag{2b}$$

Note that (2) defines n algebraic constraints that the pack model must satisfy at each point in time. It is these algebraic equations that give rise to descriptor dynamics

$$EX_{k+1} = AX_k + Bu_k + D\Theta(X_k), \tag{3a}$$

$$y_k = HX_k + \Phi(X_k), \tag{3b}$$

where $X_k = [X_{d,k}\quad X_{a,k}]^T \in \mathbb{R}^{4n}$, $X_{d,k} \in \mathbb{R}^{3n}$ represents the differential states and $X_{a,k} \in \mathbb{R}^n$ represents the algebraic states with $X_{d,k} = [x_{1,k}\ x_{2,k}\ \ldots\ x_{n,k}]^T$, and $X_{a,k} = [I_{1,k}\ I_{2,k}\ \ldots\ I_{n,k}]^T$.

y_k is the set of output vectors for n cells in parallel and is given by $y_k = [y_{1,k}\, y_{2,k}\, \cdots\, y_{n,k}]^T \in \mathbb{R}^n$, and the control input $u_k = I_k$, where I_k is the total applied input current.

As the parallel pack dynamics include both algebraic, (2), and dynamic, (1), equations the matrix E is singular. Specifically, matrices E and A are structured as

$$E = \begin{bmatrix} \mathbb{I}_{3n} & 0_{3n\times n} \\ 0_{n\times 3n} & 0_{n\times n} \end{bmatrix}, A = \begin{bmatrix} A_{11} & A_{12} \\ A_{21} & A_{22} \end{bmatrix},$$

with $\mathbb{I}_m$ being the identity matrix of dimension m and $A_{11} = diag(\tilde{A}_1,\ \tilde{A}_2,\ \cdots,\tilde{A}_n)$, $A_{12} = diag(\tilde{B}_1,\ \tilde{B}_2,\ \cdots,\tilde{B}_n)$,

$$A_{21} = \begin{bmatrix} \tilde{C}_1 & \tilde{C}_2 & 0 & \cdots & 0 \\ \tilde{C}_1 & 0 & \tilde{C}_2 & \cdots & 0 \\ \vdots & \vdots & \vdots & \ddots & \vdots \\ \tilde{C}_1 & 0 & 0 & \cdots & \tilde{C}_2 \\ 0 & 0 & 0 & \cdots & 0 \end{bmatrix} \in \mathbb{R}^{n\times 3n},$$

$\tilde{C}_1 = [0\ -1\ -1]$ and $\tilde{C}_2 = [0\ \ 1\ \ 1]$,

$$A_{22} = \begin{bmatrix} -R_{01} & (r_2+R_{02}) & 0 & \cdots & 0 \\ -R_{01} & 0 & (r_3+R_{03}) & \cdots & 0 \\ \vdots & \vdots & \vdots & \ddots & \vdots \\ -R_{01} & 0 & 0 & \cdots & (r_n+R_{0n}) \\ 1 & 1 & 1 & \cdots & 1 \end{bmatrix},$$

$B = \begin{bmatrix} 0_{4n-1} \\ -1 \end{bmatrix}$, and $D = \begin{bmatrix} 0_{3n} \\ \mathbb{I}_{n-1} \\ 0 \end{bmatrix}$.

Function $\Theta(X_k)$ contains the nonlinear part of system (3), which is imposed from Kirchhoff's laws and is given by

$$\Theta(X_k) = \begin{bmatrix} V_{OCV_{1,k}} - V_{OCV_{2,k}} \\ \vdots \\ V_{OCV_{1,k}} - V_{OCV_{n,k}} \end{bmatrix}.$$

The output (3b) models the voltage of each cell of a parallel connected battery pack with $H = [H_d \quad H_a]$, where $H_d = diag(\tilde{C}_1,\ \tilde{C}_2,\ \cdots,\ \tilde{C}_n) \in \mathbb{R}^{n\times 3n}$ and $H_a = diag(-R_{01},\ -R_{02},\cdots,\ -R_{0n}) \in \mathbb{R}^{n\times n}$, $\Phi(X_k) = [V_{OCV_{1,k}}\ \cdots\ V_{OCV_{n,k}}]^T$. Note A_{22} is a full-rank matrix, and so the linear part of the descriptor system (3) is regular and impulse-free.

Assumption 1: The nonlinear functions $\Theta(X_k)$ and $\Phi(X_k)$ are assumed to be globally Lipschitz with respect to X_k with Lipschitz constants, $\gamma_\Theta > 0$, and $\gamma_\Phi > 0$, *i.e.,*

$$||\Theta(X_1) - \Theta(X_2)|| \le \gamma_\Theta ||X_1 - X_2||, \forall X_1, X_2 \in \mathbb{R}^n, \tag{4a}$$

$$||\Phi(X_1) - \Phi(X_2)|| \le \gamma_\Phi ||X_1 - X_2||, \forall X_1, X_2 \in \mathbb{R}^n. \tag{4b}$$

Moreover, since the matrix E is rank deficient, *i.e.,* $\text{rank}(E) = 3n < 4n$, there always exists a full row rank matrix $E^\perp \in \mathbb{R}^{s\times 4n}$ such that $E^\perp E = 0$. In light of this, (3) becomes

$$\begin{bmatrix} -E^\perp B u_k \\ y_k \end{bmatrix} = \begin{bmatrix} E^\perp A \\ H \end{bmatrix} X_k + \begin{bmatrix} E^\perp D & 0 \\ 0 & \mathbb{I}_n \end{bmatrix} \begin{bmatrix} \Theta(X_k) \\ \Phi(X_k) \end{bmatrix}. \tag{5}$$

III. State Observer Design

We consider the following observer for estimating the states of system (3)

$$\xi_{k+1} = N\xi_k + F\left(\begin{bmatrix} -E^\perp B u_k \\ y_k \end{bmatrix} - \begin{bmatrix} E^\perp D & 0 \\ 0 & \mathbb{I}_n \end{bmatrix} \begin{bmatrix} \Theta(\hat{X}_k) \\ \Phi(\hat{X}_k) \end{bmatrix} \right) + Ju_k + TD\Theta(\hat{X}_k), \tag{6a}$$

$$\hat{X}_k = P\xi_k + M\left(\begin{bmatrix} -E^\perp B u_k \\ y_k \end{bmatrix} - \begin{bmatrix} E^\perp D & 0 \\ 0 & \mathbb{I}_n \end{bmatrix} \begin{bmatrix} \Theta(\hat{X}_k) \\ \Phi(\hat{X}_k) \end{bmatrix} \right), \tag{6b}$$

where $\xi_k \in \mathbb{R}^{q_0}$ is the observer state, and $\hat{X}_k \in \mathbb{R}^{4n}$ is the estimate of X_k. N, F, J, T, P and M are the unknown matrices of appropriate dimension, which must be determined such that $\hat{X}_k$ converges asymptotically to X_k.

Lemma 1: The observer (6) asymptotically estimates X_k in system (3) if there exist a matrix T of appropriate dimension such that the following conditions hold:

(a) $NTE + F\begin{bmatrix} E^\perp A \\ H \end{bmatrix} = TA$,

(b) $PTE + M\begin{bmatrix} E^\perp A \\ H \end{bmatrix} = \mathbb{I}_{4n}$,

(c) $J = TB$,

(d) The following descriptor system is asymptotically stable:

$$\mathbb{E}\eta_{k+1} = \mathbb{A}\eta_k + \mathbb{B}\delta, \tag{7}$$

where, $\eta_k = \begin{bmatrix} \varepsilon_k \\ e_k \end{bmatrix}$, $\delta = \begin{bmatrix} \Delta\Theta \\ \Delta\Phi \end{bmatrix}$, $\Delta\Theta = \Theta(X_k) - \Theta(\hat{X}_k)$, $\Delta\Phi = \Phi(X_k) - \Phi(\hat{X}_k)$,

$\mathbb{E} = \begin{bmatrix} \mathbb{I} & 0 \\ 0 & 0 \end{bmatrix}$, $\mathbb{A} = \begin{bmatrix} N & 0 \\ P & -\mathbb{I} \end{bmatrix}$, and $\mathbb{B} = \begin{bmatrix} F\begin{bmatrix} E^\perp D \\ 0 \end{bmatrix} - TD & F\begin{bmatrix} 0 \\ \mathbb{I}_n \end{bmatrix} \\ M\begin{bmatrix} E^\perp D \\ 0 \end{bmatrix} & M\begin{bmatrix} 0 \\ \mathbb{I}_n \end{bmatrix} \end{bmatrix}$.

Proof: Let $e_k = X_k - \hat{X}_k$ be the estimation error and $\varepsilon_k = \xi_k - TEX_k$ be the transformation error. Then the dynamics of ε_k is given by,

$$\varepsilon_{k+1} = N\varepsilon_k + (J - TB)u_k + \left(NTE + F\begin{bmatrix} E^\perp A \\ H \end{bmatrix} - TA \right) X_k + \left(\begin{bmatrix} F\begin{bmatrix} E^\perp D \\ 0 \end{bmatrix} - TD \end{bmatrix} \quad F\begin{bmatrix} 0 \\ \mathbb{I}_n \end{bmatrix} \right) \begin{bmatrix} \Delta\Theta \\ \Delta\Phi \end{bmatrix}. \tag{8}$$

From the definition of ε_k, (6b) can be written as,

$$\hat{X}_k = P\varepsilon_k + \left(PTE + M\begin{bmatrix} E^\perp A \\ H \end{bmatrix} \right) X_k + \left(M\begin{bmatrix} E^\perp D \\ 0 \end{bmatrix} \quad M\begin{bmatrix} 0 \\ \mathbb{I}_n \end{bmatrix} \right) \begin{bmatrix} \Delta\Theta \\ \Delta\Phi \end{bmatrix}. \tag{9}$$

If the conditions, $(a) - (c)$ of Lemma 1 are satisfied, then we obtain system (7), which must be asymptotically stable. This completes the proof. ■

A. Observer Parameterization

Define,

$$\Upsilon = \begin{bmatrix} \Gamma \\ E^{\perp}A \\ H \end{bmatrix} \text{ and } \quad \Psi = \begin{bmatrix} E \\ E^{\perp}A \\ H \end{bmatrix},$$

where $\Gamma \in \mathbb{R}^{q_0 \times 4n}$ is a full row rank matrix such that Υ is of full rank. From condition (b) of Lemma 1, we have

$$[P \quad M] \begin{bmatrix} TE \\ E^{\perp}A \\ H \end{bmatrix} = \mathbb{I}_{4n}, \tag{10}$$

which has a solution if and only if

$$\text{rank} \begin{bmatrix} TE \\ E^{\perp}A \\ H \end{bmatrix} = 4n.$$

Let $\text{rank} \begin{bmatrix} \Gamma \\ E^{\perp}A \\ H \end{bmatrix} = \text{rank} \begin{bmatrix} TE \\ E^{\perp}A \\ H \end{bmatrix} = 4n$, then there always exists a matrix $\mathscr{K} \in \mathbb{R}^{q_0 \times n}$ such that:

$$TE + \mathscr{K} \begin{bmatrix} E^{\perp}A \\ H \end{bmatrix} = \Gamma, \tag{11}$$

which can be rewritten as,

$$\begin{bmatrix} T & \mathscr{K} \end{bmatrix} \Psi = \Gamma, \tag{12}$$

and since $\text{rank} \begin{bmatrix} \Psi \\ \Gamma \end{bmatrix} = \text{rank}(\Psi)$, the solution of (12) is

$$\begin{bmatrix} T & \mathscr{K} \end{bmatrix} = \Gamma \Psi^{+}, \tag{13}$$

where Ψ^{+} denotes the Moore-Penrose (MP) inverse of Ψ. Therefore,

$$T = \Gamma \Psi^{+} \begin{bmatrix} \mathbb{I}_{4n} \\ 0 \end{bmatrix} \quad \text{and} \quad \mathscr{K} = \Gamma \Psi^{+} \begin{bmatrix} 0 \\ \mathbb{I}_{n} \end{bmatrix}. \tag{14}$$

Also, from (11), we have

$$\begin{bmatrix} TA \\ E^{\perp}A \\ H \end{bmatrix} = \begin{bmatrix} \mathbb{I}_{q_0} & -\mathscr{K} \\ 0 & \mathbb{I}_{n} \end{bmatrix} \Upsilon. \tag{15}$$

Consequently, by using (15) and (10), we obtain

$$\begin{bmatrix} P & M \end{bmatrix} \begin{bmatrix} \mathbb{I}_{q_0} & -\mathscr{K} \\ 0 & \mathbb{I}_{n} \end{bmatrix} \Upsilon = \mathbb{I}_{4n}. \tag{16}$$

The general solution of (16) is given by:

$$[P \quad M] = \left(\Upsilon^{+} - Y_2[\mathbb{I}_n - \Upsilon\Upsilon^{+}]\right) \begin{bmatrix} \mathbb{I}_{q_0} & \mathscr{K} \\ 0 & \mathbb{I}_{n} \end{bmatrix},$$

where Y_2 is an arbitrary matrix of appropriate dimension. Without loss of generality, assume that $Y_2 = 0$, then the value of P and M are obtained as

$$P = \Upsilon^{+} \begin{bmatrix} \mathbb{I}_{q_0} \\ 0 \end{bmatrix}, \tag{17}$$

$$M = \Upsilon^{+} \begin{bmatrix} \mathscr{K} \\ \mathbb{I}_{n} \end{bmatrix}. \tag{18}$$

On the other hand, by using (11), condition (a) of Lemma 1 can be rewritten as:

$$N\Gamma + (F - N\mathscr{K}) \begin{bmatrix} E^{\perp}A \\ H \end{bmatrix} = TA, \tag{19}$$

or,

$$\begin{bmatrix} N & \bar{\mathscr{K}} \end{bmatrix} \Upsilon = TA, \tag{20}$$

where $\bar{\mathscr{K}} = F - N\mathscr{K}$. The general solution of (20) is given by

$$\begin{bmatrix} N & \bar{\mathscr{K}} \end{bmatrix} = TA\Upsilon^{+} - Y_1(\mathbb{I}_{q_0+n} - \Upsilon\Upsilon^{+}), \tag{21}$$

where Y_1 is a matrix of appropriate dimension. From (21), the matrix N and $\bar{\mathscr{K}}$ are obtained as

$$N = N_1 - Y1N_2, \tag{22}$$

$$\bar{\mathscr{K}} = \bar{\mathscr{K}_1} - Y1\bar{\mathscr{K}_2}, \tag{23}$$

where, $N_1 = TA\Upsilon^{+} \begin{bmatrix} \mathbb{I}_{q_0} \\ 0 \end{bmatrix}$, $N_2 = (\mathbb{I}_{q_0+n} - \Upsilon\Upsilon^{+}) \begin{bmatrix} \mathbb{I}_{q_0} \\ 0 \end{bmatrix}$, $\bar{\mathscr{K}_1} = TA\Upsilon^{+} \begin{bmatrix} 0 \\ \mathbb{I}_{n} \end{bmatrix}$, and $\bar{\mathscr{K}_2} = (\mathbb{I}_{q_0+n} - \Upsilon\Upsilon^{+}) \begin{bmatrix} 0 \\ \mathbb{I}_{n} \end{bmatrix}$. Using the values of N and $\bar{\mathscr{K}}$ from (22) and (23), the value of matrix F is obtained as

$$\begin{aligned} F =& \bar{\mathscr{K}} + N\mathscr{K}, \\ =& \bar{\mathscr{K}_1} - Y_1\bar{\mathscr{K}_2} + (N_1 - Y_1N_2)\mathscr{K}, \\ =& F_1 - Y1F_2, \end{aligned} \tag{24}$$

where $F_1 = TA\Upsilon^{+} \begin{bmatrix} \mathscr{K} \\ \mathbb{I}_{n} \end{bmatrix}$, and $F_2 = (\mathbb{I}_{q_0+n} - \Upsilon\Upsilon^{+}) \begin{bmatrix} \mathscr{K} \\ \mathbb{I}_{q_0} \end{bmatrix}$. Now, by using the values of matrices N, F, P, and M, the descriptor system given by (7) can be written as,

$$\mathbb{E}\eta_{k+1} = \begin{bmatrix} N_1 - Y_1N_2 & 0 \\ P & \mathbb{I}_{4n} \end{bmatrix} \eta_k + \begin{bmatrix} \mathbb{F}_1 - Y_1\mathbb{F}_2 \\ \mathbb{M} \end{bmatrix} \delta, \tag{25}$$

where $\mathbb{F}_1 = \begin{bmatrix} F_1 \begin{bmatrix} E^{\perp}D \\ 0 \end{bmatrix} - TD & F_1 \begin{bmatrix} 0 \\ \mathbb{I}_{n} \end{bmatrix} \end{bmatrix}$, $\mathbb{F}_2 = \begin{bmatrix} F_2 \begin{bmatrix} E^{\perp}D \\ 0 \end{bmatrix} & F_2 \begin{bmatrix} 0 \\ \mathbb{I}_{n} \end{bmatrix} \end{bmatrix}$, and $\mathbb{M} = \begin{bmatrix} M \begin{bmatrix} E^{\perp}D \\ 0 \end{bmatrix} & M \begin{bmatrix} 0 \\ \mathbb{I}_{n} \end{bmatrix} \end{bmatrix}$.

The problem is now reduced to finding the matrix Y_1 such that the descriptor system given by (25) is asymptotically stable.

B. Stability Analysis

Theorem 1: Under Assumption 1, there exists a matrix Y_1 and a constant $\mu > 0$, such that the descriptor system given by (25) is asymptotically stable if there exists a positive definite matrix $\mathscr{U}_1 = \begin{bmatrix} \mathscr{U}_a & 0 \\ 0 & \mathscr{U}_b \end{bmatrix}$ and a symmetric matrix $\mathscr{U}_2$ such that the following LMI is satisfied

$$\begin{bmatrix} \Pi_{11} & * & * \\ 0 & -\mu\mathbb{I} & * \\ \Pi_{31} & \Pi_{32} & -\Omega \end{bmatrix} < 0,$$

where $\Omega = \mathscr{U}_1 - \mathbb{E}^{\perp T}\mathscr{U}_2\mathbb{E}^{\perp}$, $\Pi_{11} = -\begin{bmatrix} \mathscr{U}_a & 0 \\ 0 & \gamma\mathbb{I}_{4n} \end{bmatrix}$

$$\Pi_{31} = \left[\begin{array}{c|c} \mathscr{U}_aN_1 - \bar{Y}_1N_2 & 0 \\ \hline (\mathscr{U}_b - \mathscr{U}_2)P & \mathscr{U}_b - \mathscr{U}_2 \end{array}\right], \tag{26}$$

and

$$\Pi_{32} = \left[\begin{array}{c|c} -\mathscr{U}_a TD + (\mathscr{U}_a F_1 - \bar{Y}_1 F_2)\begin{bmatrix} E^{\perp} D \\ 0 \end{bmatrix} & (\mathscr{U}_a F_1 - \bar{Y}_1 F_2)\begin{bmatrix} 0 \\ \mathbb{I}_n \end{bmatrix} \\ \hline (\mathscr{U}_b - \mathscr{U}_2) M \begin{bmatrix} E^{\perp} D \\ 0 \end{bmatrix} & (\mathscr{U}_b - \mathscr{U}_2)\begin{bmatrix} 0 \\ \mathbb{I}_n \end{bmatrix} \end{array}\right]. \tag{27}$$

Proof: Consider a Lyapunov function candidate $\mathscr{V}_k = \eta_k^T \mathbb{E}^T \Omega \mathbb{E} \eta_k$, where $\Omega = \mathscr{U}_1 - \mathbb{E}^{\perp T} \mathscr{U}_2 \mathbb{E}^{\perp}$, $\mathscr{U}_1 = \begin{bmatrix} \mathscr{U}_a & 0 \\ 0 & \mathscr{U}_b \end{bmatrix} > 0$ and $\mathscr{U}_2$ be a symmetric matrix. Then, using (7), the rate of variation $\Delta\mathscr{V}$ of this Lyapunov function candidate is given by

$$\begin{aligned} \Delta\mathscr{V} &= \mathscr{V}_{k+1} - \mathscr{V}_k \\ &= \eta_{k+1}^T \mathbb{E}^T \Omega \mathbb{E} \eta_{k+1} - \eta_k^T \mathbb{E}^T \Omega \mathbb{E} \eta_k \\ &= (\mathbb{A}\eta_k + \mathbb{B}\delta)^T \Omega (\mathbb{A}\eta_k + \mathbb{B}\delta) - \eta_k^T \mathbb{E}^T \Omega \mathbb{E} \eta_k \\ &= \eta_k^T \mathbb{A}^T \Omega \mathbb{A} \eta_k + \eta_k^T \mathbb{A}^T \Omega \mathbb{B} \delta + \delta^T \mathbb{B}^T \Omega \mathbb{A} \eta_k \\ &+ \delta^T \mathbb{B}^T \Omega \mathbb{B} \delta - \eta_k^T \mathbb{E}^T \Omega \mathbb{E} \eta_k + \delta^T \mu \delta - \delta^T \mu \delta. \end{aligned} \tag{28}$$

From the Lipschitz condition (4), we have

$$\begin{aligned} \delta^T \mu \delta &= \Delta\Theta^T \mu \Delta\Theta + \Delta\Phi^T \mu \Delta\Phi \\ &\leq \mu \gamma_\Theta^2 e_k^T e_k + \mu \gamma_\Phi^2 e_k^T e_k \\ &\leq \eta_k^T \begin{bmatrix} 0 & 0 \\ 0 & \gamma \mathbb{I}_{4n} \end{bmatrix} \eta_k, \end{aligned} \tag{29}$$

where $\mu > 0$ is a scaler and $\gamma = \mu(\gamma_\Theta^2 + \gamma_\Phi^2)$. Using (29), (28) can be rewritten as

$$\begin{aligned} \Delta\mathscr{V} \leq \eta_k^T \left(\mathbb{A}^T \Omega \mathbb{A} - \mathbb{E}^T \Omega \mathbb{E} + \begin{bmatrix} 0 & 0 \\ 0 & \gamma \mathbb{I}_{4n} \end{bmatrix} \right) \eta_k + \eta_k^T \mathbb{A}^T \Omega \mathbb{B} \delta \\ + \delta^T \mathbb{B}^T \Omega \mathbb{A} \eta_k + \delta^T (\mathbb{B}^T \Omega \mathbb{B} - \mu \mathbb{I}) \delta, \end{aligned} \tag{30}$$

which can further be rewritten as,

$$\Delta\mathscr{V} \leq \begin{bmatrix} \eta_k \\ \delta \end{bmatrix}^T \Pi \begin{bmatrix} \eta_k \\ \delta \end{bmatrix}, \tag{31}$$

where $\Pi = \begin{bmatrix} \mathbb{A}^T \Omega \mathbb{A} - \mathbb{E}^T \Omega \mathbb{E} + \begin{bmatrix} 0 & 0 \\ 0 & \gamma \mathbb{I}_{4n} \end{bmatrix} & \mathbb{A}^T \Omega \mathbb{B} \\ \mathbb{B}^T \Omega \mathbb{A} & \mathbb{B}^T \Omega \mathbb{B} - \mu \mathbb{I} \end{bmatrix}$. If the LMI, $\Pi < 0$, then $\Delta\mathscr{V} < 0$. Taking Schur complement of the LMI, Π, we get

$$\begin{bmatrix} -\mathbb{E}^T \Omega \mathbb{E} + \begin{bmatrix} 0 & 0 \\ 0 & \gamma \mathbb{I}_{4n} \end{bmatrix} & 0 & \mathbb{A}^T \Omega \\ 0 & -\mu \mathbb{I} & \mathbb{B}^T \Omega \\ \Omega \mathbb{A} & \Omega \mathbb{B} & -\Omega \end{bmatrix} < 0. \tag{32}$$

By putting the value of Ω in (32), we find the values of the individual terms of Π as follows:

$$\Pi_{11} = -\mathbb{E}^T \Omega \mathbb{E} + \begin{bmatrix} 0 & 0 \\ 0 & \gamma \mathbb{I}_{4n} \end{bmatrix} = -\begin{bmatrix} \mathscr{U}_a & 0 \\ 0 & \gamma \mathbb{I}_{4n} \end{bmatrix},$$

$$\Pi_{31} = \Omega \mathbb{A} = (\mathscr{U}_1 - \mathbb{E}^{\perp T} \mathscr{U}_2 \mathbb{E}^{\perp}) \begin{bmatrix} N_1 - Y_1 N_2 & 0 \\ P & \mathbb{I}_{4n} \end{bmatrix},$$

$\Pi_{32} = \Omega \mathbb{B} = (\mathscr{U}_1 - \mathbb{E}^{\perp T} \mathscr{U}_2 \mathbb{E}^{\perp}) \begin{bmatrix} \mathbb{F}_1 - Y_1 \mathbb{F}_2 \\ \mathbb{M} \end{bmatrix}$, which on further simplifying, reduces to (26) and (27), respectively. The matrix, Y_1 is then obtained as $Y_1 = \mathscr{U}_a^{-1} \bar{Y}_1$. This completes the proof. ■

IV. Results and Discussion

To simplify the presentation of results, and without loss of generality, we consider two cells connected in parallel for the simulations. While the cells differ in their model parameters, they share the same SOC-OCV relationship, given by

$$\begin{aligned} V_{OCV}(Z_{m,k}) =& 3.684 + 0.175 Z_{m,k} + 0.068 {Z_{m,k}}^2 + 0.048 {Z_{m,k}}^3 \\ &- 0.010 {Z_{m,k}}^4 - 0.006 {Z_{m,k}}^5. \end{aligned} \tag{33}$$

The model parameters for both cells are listed in Table I, with the busbar resistance set to 0.02Ω.

TABLE I: ECM Parameters used in Simulation Study

	Cell 1	Cell 2	Units
R_0	0.040	0.030	[Ω]
R_1	0.095	0.090	[Ω]
C_1	30000	25000	[F]
R_2	0.075	0.070	[Ω]
C_2	50000	45000	[F]
C_b	2.6	2.4	[Ah]

As shown in Fig. 2, the total current (a) is unevenly distributed between the cells due to inherent cell heterogeneities, a behaviour further detailed in Fig. 2(b). However, when the busbar resistance is included in the model, the current mismatch between the two cells becomes even more pronounced, as seen in Fig. 2(c). In particular, with the inclusion of busbar resistance of 0.02Ω, the mismatch in currents grew by 9.69% for cell 1 and by 8.55% for cell 2. This increased current disparity is a direct consequence of the voltage drops across the busbar, which further exacerbates the impact of cell-to-cell variations. Without accounting for busbar resistance, the model underestimates the degree of current mismatch, potentially leading to an inaccurate representation of the operational stress on each cell. Including the busbar resistance highlights the importance of considering interconnection resistances within the pack, as they significantly influence current sharing and can lead to uneven degradation over time if neglected.

Now, we proceed to apply our proposed observer to this two-cell pack. We begin by fixing the order of the observer as $q_0 = 5$ and selecting matrix

$$\Gamma = \begin{bmatrix} 1 & 1 & 1 & 0 & 0 & 1 & 1 & 0 \\ 0 & 1 & 1 & 0 & 0 & 1 & 1 & 0 \\ 1 & 0 & 1 & 0 & 1 & 1 & 0 & 0 \\ 0 & 0 & 0 & 1 & 0 & 0 & 0 & 0 \\ 1 & 0 & 1 & 1 & 1 & 1 & 0 & 1 \end{bmatrix},$$

such that Υ is full column rank matrix. Then, solving LMI (32), we obtain the matrix Y_1 as follows:

$$Y_1 = \begin{bmatrix} 0.042 & -0.253 & -1.642 & -0.243 & -1.488 & -0.343 & 0.384 & 0.104 & 0.448 \\ 0.142 & 0.054 & -0.213 & -0.094 & -0.306 & 0.008 & 0.043 & 0.037 & 0.029 \\ -0.097 & -0.306 & -1.432 & -0.150 & -1.188 & -0.351 & 0.341 & 0.068 & 0.420 \\ 0.108 & 0.332 & 1.547 & 0.161 & 1.280 & 0.381 & -0.368 & -0.073 & -0.454 \\ -0.135 & -0.028 & 0.334 & 0.107 & 0.407 & 0.021 & -0.072 & -0.043 & -0.064 \end{bmatrix}.$$

This matrix is then used to calculate the other observer matrices, as discussed in detail in Section III-A.

In order to estimate the SOC and local currents of the two-cell pack considered in the simulation study, we initialize the observer as $\xi_0 = [0.5\ 0\ 0\ 0.55\ 0\ 0\ -3\ -3]^T$. Figs.

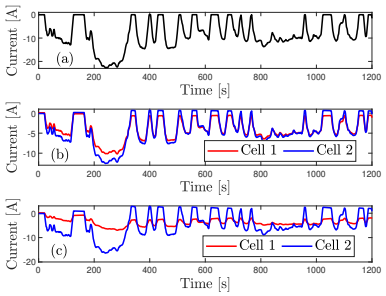

Fig. 2: (a) Total current, (b) current distribution without busbar resistance and (c) with busbar resistance

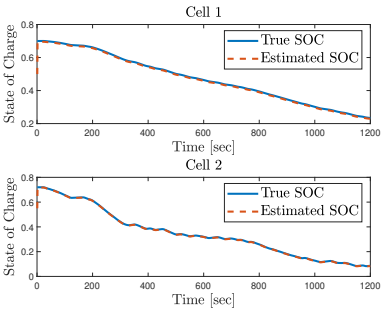

Fig. 3: Comparison of true SOC with its estimated value

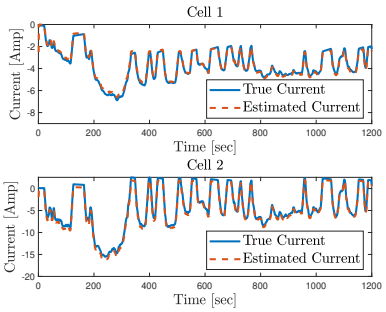

Fig. 4: Comparison of true current with its estimated value

3 and 4 show the true and estimated values of SOC and the local currents for both cells 1 and 2. As evident from these figures, the observer effectively recovers the states quickly, even when starting from large initial errors. This rapid convergence to accurate estimates confirms the theoretical predictions of asymptotic zero error convergence, as established in Theorem 1. These results highlight the effectiveness of the observer in accurately estimating the states of the battery pack, underscoring its practical utility in real-world applications.

V. Conclusion

In this paper, an observer for a parallel-connected lithium-ion battery was proposed. The observer was defined for the nonlinear descriptor dynamics of the pack, and stability conditions for the estimation error were stated. When evaluated on the UDDS discharge cycle, the observer was shown to perform well with RMSEs of 0.0072 and 0.0054 for the SOCs as well as $0.3A$ and $0.28A$ for the currents in cells 1 and 2, respectively. Moreover, the results also demonstrated the importance of including busbar resistances into the model, as a busbar resistance of 0.02Ω was shown to increase the current mismatch by 9.69% for cell 1 and by 8.55% for cell 2. The goal of these results is to demonstrate the potential of cell-level state estimation for battery management systems designed to control every cell in the large packs powering the next generation of electric technologies.

References

[1] G. L. Plett, *Battery management systems, Volume II: Equivalent-circuit methods*. Artech House, 2015.

[2] A. Fill, S. Koch, and K. P. Birke, "Algorithm for the detection of a single cell contact loss within parallel-connected cells based on continuous resistance ratio estimation," *Journal of Energy Storage*, vol. 27, p. 101049, 2020.

[3] D. Beck, P. Dechent, M. Junker, D. U. Sauer, and M. Dubarry, "Inhomogeneities and cell-to-cell variations in lithium-ion batteries, a review," *Energies*, vol. 14, no. 11, p. 3276, 2021.

[4] A. M. Bizeray, S. Zhao, S. R. Duncan, and D. A. Howey, "Lithium-ion battery thermal-electrochemical model-based state estimation using orthogonal collocation and a modified extended Kalman filter," *Journal of Power Sources*, vol. 296, pp. 400–412, 2015.

[5] R. Drummond, L. D. Couto, and D. Zhang, "Resolving Kirchhoff's laws for parallel Li-ion battery pack state-estimators," *IEEE Transactions on Control Systems Technology*, vol. 30, no. 5, pp. 2220–2227, 2021.

[6] Z. Li, A. Zuo, Z. Mo, M. Lin, C. Wang, J. Zhang, M. H. Hofmann, and A. Jossen, "Demonstrating stability within parallel connection as a basis for building large-scale battery systems," *Cell Reports Physical Science*, vol. 3, no. 12, 2022.

[7] A. Weng, H. Movahedi, C. Wong, J. B. Siegel, and A. Stefanopoulou, "Current imbalance in dissimilar parallel-connected batteries and the fate of degradation convergence," *J. Dyn. Syst. Meas. Control*, vol. 146, p. 011106, 2024.

[8] T. Bruen and J. Marco, "Modelling and experimental evaluation of parallel connected lithium ion cells for an electric vehicle battery system," *Journal of Power Sources*, vol. 310, pp. 91–101, 2016.

[9] J. A. Lone, R. Drummond, S. Bhaumik, and N. K. Tomar, "Cell-level state-estimation in parallel connected lithium-ion battery packs," *Submitted to IEEE Transactions on Transportion Electrification*, 2024.

[10] S. Meng, F. Meng, F. Zhang, Q. Li, Y. Zhang, and A. Zemouche, "Observer design method for nonlinear generalized systems with nonlinear algebraic constraints with applications," *Automatica*, vol. 162, p. 111512, 2024.

[11] T. Berger and T. Reis, "ODE observers for DAE systems," *IMA Journal of Mathematical Control and Information*, vol. 36, no. 4, pp. 1375–1393, 2019.

[12] J. Jaiswal and N. K. Tomar, "Existence conditions for ODE functional observer design of descriptor systems," *IEEE Control Systems Letters*, vol. 6, pp. 355–360, 2021.

[13] Z. Wang, Y. Shen, X. Zhang, and Q. Wang, "Observer design for discrete-time descriptor systems: An LMI approach," *Systems & Control Letters*, vol. 61, no. 6, pp. 683–687, 2012.

[14] D. Coutinho, C. E. de Souza, M. Kinnaert, and S. Schons, "Robust observer design for a class of discrete-time nonlinear singular systems with persistent disturbances," *International Journal of Adaptive Control and Signal Processing*, vol. 35, no. 1, pp. 51–68, 2021.

[15] J. A. Lone, N. K. Tomar, and S. Bhaumik, "Functional observer design for parallel connected Li-ion battery: A descriptor systems theory approach," *IEEE Control Systems Letters*, vol. 7, pp. 961–966, 2022.

[16] J. A. Lone, A. Goel, N. K. Tomar, and S. Bhaumik, "Kalman filtering for descriptor systems: An alternative approach and application to cell level estimation of a lithium-ion battery," in *Procs. of the Conference on Decision and Control (CDC)*. IEEE, 2023, pp. 2570–2575.

[17] D. Zhang, L. D. Couto, S. Benjamin, W. Zeng, D. F. Coutinho, and S. J. Moura, "State of charge estimation of parallel connected battery cells via descriptor system theory," in *Proceedings of the American Control Conference (ACC)*. IEEE, 2020, pp. 2207–2212.

[18] J. M. Reniers and D. A. Howey, "Digital twin of a MWh-scale grid battery system for efficiency and degradation analysis," *Applied Energy*, vol. 336, p. 120774, 2023.